# Adaptive Fuzzy Game-based Energy Efficient Localization in 3D Underwater Sensor Networks

YALI YUAN*, University of Goettingen, Germany
CHENCHENG LIANG*, Uppsala University, Sweden
XU CHEN, Sun Yat-sen University, China
THAR BAKER, Liverpool John Moores University, United Kingdom
XIAOMING FU, University of Goettingen, Germany

Numerous applications in 3D underwater sensor networks (UWSNs), such as pollution detection, disaster prevention, animal monitoring, navigation assistance, and submarines tracking, heavily rely on accurate localization techniques. However, due to the limited batteries of sensor nodes and the difficulty for energy harvesting in UWSNs, it is challenging to localize sensor nodes successfully within a short sensor node lifetime in an unspecified underwater environment. Therefore, we propose the Adaptive Energy-Efficient Localization Algorithm (Adaptive EELA) to enable energy-efficient node localization while adapting to the dynamic environment changes. Adaptive EELA takes a fuzzy game-theoretic approach, whereby Stackelberg game is used to model the interactions among sensor and anchor nodes in UWSNs and employs the adaptive neuro-fuzzy method to set the appropriate utility functions. We prove that a socially optimal Stackelberg–Nash Equilibrium is achieved in Adaptive EELA. Through extensive numerical simulations under various environmental scenarios, the evaluation results show that our proposed algorithm accomplishes a significant energy reduction, e.g., 66% lower compared to baselines, while achieving a desired performance level in terms of localization coverage, error, and delay.

CCS Concepts: • **Networks → Location based services**; **Network design principles**.

Additional Key Words and Phrases: Underwater sensor networks, localization, adaptive EELA, dynamic environment, energy consumption, localization coverage

**ACM Reference Format:**
Yali Yuan, Chencheng Liang, Xu Chen, Thar Baker, and Xiaoming Fu. 2020. Adaptive Fuzzy Game-based Energy Efficient Localization in 3D Underwater Sensor Networks. 1, 1 (October 2020), 19 pages. https://doi.org/xxxxx

## 1 INTRODUCTION

Localization of underwater sensor nodes is useful in numerous applications, such as climate monitoring, disaster prevention, marine life researches and unknown mineral exploration. In such applications, only the location-aware data are useful in the real world. Nonetheless, UWSNs employ the acoustic communication systems and are constrained

*Both authors contributed equally to this research.

Authors' addresses: Yali Yuan, Corresponding-email:yali.yuan@cs.uni-goettingen.de, University of Goettingen, Goldschmidtstraße 7, Goettingen, Germany, 37077; Chencheng Liang, chencheng.liang@it.uu.se, Uppsala University, Uppsala, Sweden, 75237; Xu Chen, chenxu35@mail.sysu.edu.cn, Sun Yat-sen University, Guangzhou, 510275, China, chenxu35@mail.sysu.edu.cn; Thar Baker, t.baker@ljmu.ac.uk, Liverpool John Moores University, United Kingdom; Xiaoming Fu, fu@cs.uni-goettingen.de, University of Goettingen, Goettingen, Germany.

by numerous factors, like bandwidth, multipath fading, energy consumption, and frequency dispersion [6, 29], which impedes the development of localization techniques in UWSNs [23, 34, 35]. The reduction of energy cost is a goal in many application fields [1, 27, 38]. The energy-efficient strategy is more critical in underwater localization systems due to the underwater nodes' limited battery storage and high replacement cost.

Besides, to perform assignments, such as location-based tracking or routing protocols, in a dynamic changing underwater environment, self-adaptation learning ability is highly demanded in designing energy-efficient localization methods for underwater nodes in UWSNs, especially for an unspecified underwater environment. Self-adaptation learning design requires a certain level of intelligence and autonomy [37]. Intelligence in localization means the localization model like humans can acquire knowledge from its own or other models' experience and apply this knowledge to improve its performance while dealing with uncertainties in underwater environments. Autonomy in localization denotes the sensor nodes can find enough anchor nodes to obtain its location. Since in most localization schemes, one sensor node needs several anchor nodes' help to obtain its location [33, 41].

So far, very few works have studied the issue of energy-efficient localization in UWSNs [25, 42]. In [25], the interaction between sensor nodes and anchor nodes is modeled using the Stackelberg game to achieve an energy-efficient localization scheme. In this scheme, the strategy is used to reduce the energy consumed by anchor nodes but with a high energy cost of sensor nodes. However, in the real world, there are usually more sensor nodes than anchor nodes, thereby for the whole network, reducing the energy consumed by sensor nodes is vital for a longer lifetime. In [42], the authors used a Stackelberg game that enabled sensor nodes to communicate with sufficient anchor nodes to calculate their locations with the least energy cost. Unlike [25], this scheme takes the energy cost of both anchor and sensor nodes into account, resulting in a reduction of the energy consumption per node. However, this scheme works efficiently only in one specific environment and predefined weights are required to set the utility functions. Once the environment such as the number of nodes or network size changes, the utility weights of this scheme need to be recalculated, which is time and energy-consuming. Although these methods show promising results, they are unable to handle dynamic variations of the network and underwater environments. Moreover, no one considers the unpredictability of the environment for localization design in UWSNs.

Considering the aforementioned issues, we propose an energy-efficient localization scheme in UWSNs with the capacity of adaptive response according to variations of the underwater environment and name it *Adaptive EELA*. In this work, we design and implement our initial work [43] in a 3D dynamic underwater environment. Adaptive EELA is designed with the consideration of a localization scenario, which consists of several sensor nodes (with unknown locations) and their surrounding neighbor anchor nodes (with known locations). It does not need prior knowledge, new devices, and other extra costs. Based on the Single-Leader-Multi-Follower Stackelberg game, the localization scenario in UWSNs is modeled, where in order to localize a single sensor node (leader) successfully, several neighboring anchor nodes (followers) are demanded. Furthermore, lacking the capacity of working in uncertain and mutative environments, the approaches mentioned in [14, 25, 42] are not suitable in the real-world. Adaptive neural fuzzy inference system (ANFIS) [15] incorporating the advantages of both neural networks and fuzzy logic with human-like reasoning strategy, provides a promising solution for the decision-making of anchor/sensor nodes in the underwater localization process. Motivated by that, in this paper, ANFIS is employed as utility functions of the proposed fuzzy game-theoretic algorithm, since different factors affect the decision of both sensor and anchor nodes to pursue the optimal transmission range during the localization process in UWSNs. For example, anchor nodes require to consider several factors including the sensor nodes' total demand, residual energy as well as number of requests from sensor nodes that can be resolved by anchor nodes in order to choose an optimal transmission range during the localization process. The adaptive neuro-fuzzy

model considered in this paper is able to express the qualitative experience and knowledge despite the uncertainty caused by these factors. In summary, we have the following contributions:

1) Adaptive EELA is proposed as a means to reduce the energy consumption of localization tasks in UWSNs. In the proposed scheme, all nodes' transmission power is optimized, by enabling the localization of a maximum number of sensor nodes with reduced energy costs.
3) With Adaptive EELA, an automatic learning algorithm in the offline phase is realized, that is just required once. After the learning, in online scenarios with the environmental uncertainties - like the density or topologies of the nodes - are able to be accommodated by Adaptive EELA.
4) Numerical evaluations covering different network topologies and density of nodes show that the average per-node energy consumed in the proposed scheme is around 66% of the referenced methods, while achieving good performances in terms of localization coverage, error, and delay.

We organized the rest content as follows: Section 2 discusses the related works. In Section 3, the Adaptive EELA scheme is described in detail. In Section 4, the results of simulation and performance evaluation are investigated. Finally, Section 5 gives the conclusion as well as future perspectives.

## 2 RELATED WORK

### 2.1 Localization in UWSNs

Localization schemes in 3D UWSNs have drawn the attention of the networking community since the 2000s. However, most proposed schemes were only suitable for a specific scenario. In [45], a hierarchical localization approach was used to improve the localization performance in large-scale UWSNs. This scheme, based on 3D-distance estimation, achieved a high localization coverage but with high computational complexity and energy consumption. 3D underwater localization was proposed in [14], where only three anchor nodes were used to initialize the localization scheme, while the sensor node's location was calculated by trilaterition algorithm according to the location information of anchor nodes. However, its localization error was accumulated with the iterations, decreasing the localization accuracy. In [13], time difference of arrival (TDoA) was used to determine the communication range. Based on that, the target node location was calculated by the trilateration technique. Then, the target node could be tracked by the obtained location and velocity in UWSNs, with a good performance. [34] computed the nodes' location based on active nodes' Received Signal Strengths (RSSs) and reduced the block kernel matrix's calculation error of the shortest path. [40] solved the asynchronous localization problem of underwater nodes by considering the propagation delay and location. The unscented Kalman filtering technique was used to optimize the localization process. However, the localization accuracy of these schemes highly depends on the application scenario. In [31], the authors solved the common issue of packet scheduling and self-localization in UWSNs. To solve the localization issues in UWSNs, like asynchronous clocks and mobility of nodes, the iterative least-squares estimators are employed for optimizing the localization issues and reducing the sum of all measurement errors [39]. Autonomous Underwater Vehicle was used as beacon nodes in some schemes [9, 10, 44], but leading to an extra cost to UWSNs.

### 2.2 Topology Control

Li et al. [17] first presented an algorithm for topology control in wireless multi-hop networks for a reduction of transmission power in global connectivity maintenance. The energy-efficient Quality of Service (QoS) topology control problem, in terms of an integer or a mixed-integer linear problem, for heterogeneous ad hoc wireless networks was

discussed in [16]. In [32], the authors proposed the joint power and topology control algorithm, where the topology control problem of heterogeneous sensor networks was built by a game-theoretical model. Three characteristics, such as reliability, connectivity, and power efficiency, were considered to improve the algorithm performance. To extend the lifetime of the network, Zhu et al. [46] employed the power control scheme based on game-theory with Hidden Markov Model (HMM) in UWSNs. Despite the increasing research interests in UWSNs, few works have been conducted on topology control methods tailored to UWSNs. A distributed radius determination algorithm was proposed in [21] to solve the topology control problem in mobile UWSNs. Simulation results showed that a well-constructed topology can be obtained. Based on complex network theory, Liu et al. [20] used a topology control strategy to select two different cluster-heads, which can lead to better network connectivity as well as the coverage area. In this strategy, the initial topology was generated randomly by a scale-free network model. In [11], node deployment strategies of localization systems in a 3D underwater environment were investigated, namely regular tetrahedron deployment, random deployment and cubic deployment.

In [25], Opportunistic Localization by Topology Control (OLTC) scheme implemented by a Single-Leader-Multi-Follower Stackelberg game was designed for better network performance, such as localization accuracy, energy consumption as well as coverage, in sparse UWSNs. Sensor nodes got their locations by trilateration algorithm based on the information of anchor nodes. However, only the energy consumption of anchor nodes was considered in OLTC, while the energy cost of sensor nodes could be much higher in real-world applications. Besides, the strict requirement for the initial nodes deployment prevented this model from a wide usage. Hence, the EELA scheme [42], which takes the energy consumption of sensor nodes into account, was proposed. A novel Stackelberg game was employed to help not all nodes for choosing the optimal transmission power in the opportunistic localization system. However, EELA is unable to adapt to different network topologies or different densities of nodes. Once the node density or the network topology changes, the optimal weights of different input parameters in utility functions would not be applicable. Instead, our proposed *adaptive EELA* is designed to cope with such dynamic changes through an efficient learning strategy.

## 3 PROBLEM FORMULATION AND SOLUTION

In a distributed localization scenario in UWSNs, multiple anchor nodes are required in order to successfully localize a sensor node. However, in real underwater scenarios, sensor nodes may not receive enough location beacons from neighboring anchor nodes because of the spare deploying nodes and the water current in UWSNs. In such a scenario, the localization process is initialized by sensor nodes, and based on their requests, anchor nodes reply by sending out beacons. This motivates us to build the interactions among anchor and sensor nodes in UWSNs by the Single-Leader-Multi-Follower Stackelberg game as in [25, 42], where sensor nodes act as leaders while anchor nodes act as followers. However, [14, 25, 42] are unsuitable for a dynamic environment. In the real-world, the decision-making of anchor nodes not only need to consider factors like the energy storage, requests of sensor nodes but also the dynamic underwater environment changes. This motivates us to propose an adaptive fuzzy game-theoretic model based on Fuzzy logic. Fuzzy logic enables us to express the qualitative information as well as uncertainties. In the sequel, the 3D deployment scenario and transmission model is introduced firstly, followed by the illustration of ANFIS design. Then, we describe and analyze the proposed Adaptive EELA model to improve the energy efficiency of nodes' localization in 3D UWSNs.

### 3.1 Deployment Scenario and Propagation Model

Fig. 1 depicts the deployment scenario, in which cylinders / dotted circles represent sensor / anchor nodes (SNs, ANs) respectively. Nodes are randomly deployed following the uniform distribution on the surface (anchor nodes) or beneath

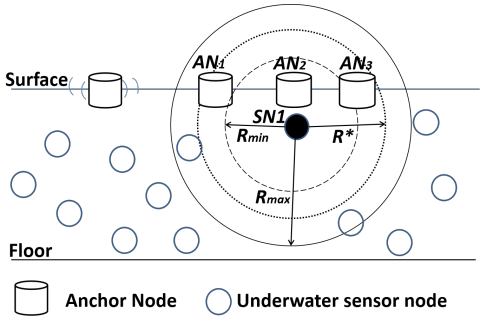


Fig. 1. 2D view of the considered 3D deployment scenario.

the surface (sensor nodes). The 3D space is of volume $L \times W \times H$ (length, width, and height). The sets of anchor and sensor nodes are defined as $\{N_a\}$ and $\{N_s\}$, respectively. Due to the influence of the underwater currents and water waves, all nodes are mobile.

For one sensor node $i$, the number of anchor nodes within its coverage with transmission power $P_i$, denoted as $n_{neig}^{P_i}$. $P_i$'s value is between $[P_{min}, P_{max}]$ and the corresponding transmission range is between $[R_{min}, R_{max}]$. $R^*$ denotes the optimal transmission range. The frequently-used symbols are listed in Table 1. We assume that anchor and sensor nodes have access to information, such as time for synchronization and depth. According to [12], the transmission power $P$ needed by a sender node to reach a receiver node at a distance $R$ and frequency $f$, is defined as,

$$P = A(R, f) + P_0, \tag{1}$$

where $P_0$ indicates the received signal strength and $A(R, f)$ denotes the signal attenuation with frequency $f$ over distance $R$ in an underwater acoustic channel. Further details can be found in [42].

### 3.2 Description of ANFIS

Adaptive EELA can be modeled as a strategic game, in which there are two different kinds of hierarchical players: one leader and some followers [36]. In this game, the leader moves first by selecting one strategy. After that, followers always choose the best strategy to maximize their benefits. Then, based on followers' reactions, the leader gives the best response to maximize its benefit. ANFIS [15] is employed to help sensor and anchor nodes making decisions for selecting their best interaction strategies based on many factors, such as the energy consumption, the number of neighboring nodes and requests.

ANFIS is implemented in the multilayer feedforward neural network, which can adapt the relationship of fuzzy variables to the changing environment for predicting the locations of sensor nodes in UWSNs. There are various features, like parameter estimation, rule extraction, and self-construction. In the Adaptive EELA scheme proposed in this paper, ANFIS is used to model its utility functions in place of the mathematical definitions in [42], and to optimize transmit power selection. Due to its learning ability and adaptability, the performance of ANFIS is superior to the conventional fuzzy logic algorithm [7].

As shown in Fig. 2, the ANFIS framework employed in this paper is an updated version based on [5], consisting of three inputs, five layers, eight fuzzy rules, and one output. Besides, it is assumed that there are two associated membership functions (MFs) for every input. Eight fuzzy if-then rules are employed. Below are two examples of them,

| Symbol | Meaning |
|---|---|
| $\{N_s\}$ | Set of sensor nodes |
| $\{N_a\}$ | Set of anchor nodes |
| $\tilde{n}_h^{req}$ | Additional number of anchor nodes needed by the $i$-th sensor node (fuzzy variable) |
| $\tilde{n}_{neig}(P_i)$ | Number of neighbor anchor nodes of $i$-th sensor node (fuzzy variable) |
| $n_{min}^{req}$ | Minimum number of anchor nodes needed for sensor node for localization |
| $N$ | Background noise |
| $\tilde{E_{tl}}$ | Total energy of the node (fuzzy variable) |
| $C_j$ | Anchor node's transmitted energy consumption per unit power |
| $E_i$ | Sensor node's transmitted energy consumption per unit power |
| $P_i$ | Sensor node's current transmission power |
| $Q_j$ | Anchor node's current transmission power |
| $\tilde{P}_i$ | Sensor node's future transmission power (fuzzy variable) |
| $\tilde{Q}_j$ | Anchor node's future transmission power (fuzzy variable) |
| $P_{max}$ | Sensor node's maximal transmission power |
| $Q_{max}$ | Anchor node's maximal transmission power |
| $\tilde{n}_{hd}(Q_j)$ | Number of sensor nodes' requests that can be resolved by $j$-th anchor node given future transmission power (fuzzy variable) |
| $n_{arx}$ | Number of sensor nodes' requests that can be resolved by anchor node with current transmission power (fuzzy variable) |
| $OA_j$ | Anchor node's localization capability |

Table 1. Table of symbols.

Rule 1: If $x$, $y$ and $z$ are $A_1$, $B_1$ and $C_1$ respectively, then $f_1 = p_1 \cdot x + q_1 \cdot y + e_1 \cdot z + r_1$,

Rule 2: If $x$, $y$ and $z$ are $A_2$, $B_2$ and $C_2$ respectively, then $f_2 = p_2 \cdot x + q_2 \cdot y + e_2 \cdot z + r_2$.

In rule 1 and 2, $f_d$ is the linear consequent function. $p_d$, $q_d$, $e_d$ and $r_d$ for $d \in \{1, 2\}$ are linear parameters of the first-order Sugeno fuzzy model.

In Fig. 2, firstly, we use the bell-shaped MFs to generate the membership grades of the inputs. The AND operator is employed to calculate the output, which is the antecedent result of a specific rule, i.e., firing strength. Then the ratio of each rule's firing strength to the sum of all rules' firing strength, is obtained in the third layer. After that, we can get the contribution of each rule toward the total output. Finally, each fuzzy rule's fuzzy results are transformed by the

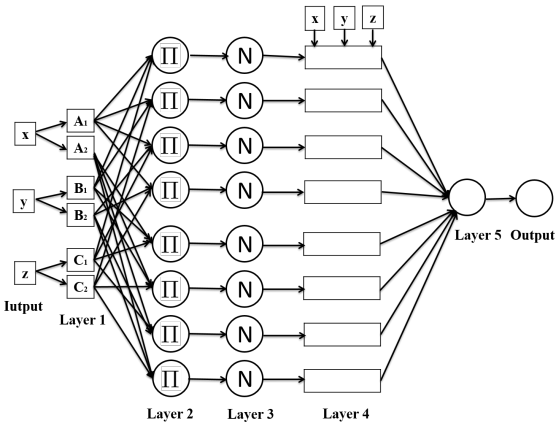


Fig. 2. ANFIS structure with three inputs and one output.

defuzzification technique into a crisp output, which are all summed to obtain the final output, i.e.,

$$\begin{aligned} O &= \sum_{d=1}^{N} \overline{w}_d f_d \\ &= \sum_{d=1}^{N} \overline{w_d}(p_d \cdot x + q_d \cdot y + h_d \cdot z + r_d), \\ &= \sum_{d=1}^{N} \overline{w}_d p_d \cdot x + \sum_{d=1}^{N} \overline{w}_d q_d \cdot y + \sum_{d=1}^{N} \overline{w}_d h_d \cdot z + \sum_{d=1}^{N} \overline{w}_d r_d, \end{aligned} \tag{2}$$

where $O$ represents the final output of ANFIS method. $\overline{w}_d$ denotes a normalized firing strength, i.e., $d$-th node's output from the former layer. $N$ equals eight in this paper. The detailed derivation for Eq. (2) can be found in [5].

For sensor nodes, $\tilde{n}_{neig}(P_i)$, $\tilde{E}_i^{tl}$ and $\sum_{h=1}^{n_{srx}} \tilde{Q}_h$ are fuzzy variables which are input parameters (see Table 1) corresponding to $x$, $y$ and $z$. Similarly, fuzzy variables are $\tilde{n}_{hd}(Q_j)$, $\tilde{E}_j^{tl}$, $\sum_{k=1}^{n_{arx}} \tilde{P}_k$ (see Table 1) for anchor nodes. The outputs are the value of the payoff of the sensor and anchor nodes. ANFIS network is designed as a supervised learning technique and trained by the dataset collected from offline simulations which reflect the real underwater scenarios. Based on this training, the goal of this ANFIS network is to adapt to varying environments by learning the adequate parameter values described above, without requiring new training phase nor data once it is deployed online.

### 3.3 Modeling and Analysis of Adaptive EELA

In the proposed Adaptive EELA, anchor nodes act as followers. Their optimal strategies are selected by serving the maximum number of sensor nodes' requests with the minimum overhead. The sensor node acts as a leader monitoring the response from the anchor nodes. According to the response from the followers, the sensor node maximizes its profit. The strategy of the leader is to find the maximum anchor nodes with the minimum energy cost. Sensor nodes will localize themselves after enough neighbor beacon locations are received.

We employ the proposed ANFIS as the utility functions of both anchor and sensor nodes to enhance different metrics like energy consumption, and the localization ability of sensor nodes by optimizing their transmission powers in a dynamic environment. In the sequel, we adopt the utility definitions of [42] but based on the new fuzzy variables inputs

as in [22]. Note that these utility definitions in Eqs. (3), (4) are weighted sums of the fuzzy variable inputs and hence are similar to the ANFIS output in Eq. (2).

Thus, the utility function of anchor node $j$ is the weighted sum of the residual energy $\left(\tilde{E}_j^{tl} - C_j Q_j\right)$ and the localization capability of the $j$-th anchor node $\tilde{OA}_j(Q_j, \tilde{P}_1, \tilde{P}_2, \cdots, \tilde{P}_{n_{arx}})$,

$$U_F(Q_j, \tilde{P}_1, \tilde{P}_2, \cdots, \tilde{P}_{n_{arx}}) = w_{1j}\left(\tilde{E}_j^{tl} - C_j Q_j\right) + w_{2j}\tilde{OA}_j(Q_j, \tilde{P}_1, \tilde{P}_2, \cdots, \tilde{P}_{n_{arx}}), \tag{3}$$

where $\tilde{E}_j^{tl}$, $\tilde{n}_{hd}(Q_j)$ and $\sum_{i=1}^{n_{arx}} \tilde{P}_i$ are the fuzzy variables $x$, $y$ and $z$. $\tilde{E}_j^{tl}$ is the current total remaining energy of the $j$-th anchor node. $\tilde{OA}_j(Q_j, \tilde{P}_1, \tilde{P}_2, \cdots, \tilde{P}_{n_{arx}})$ is computed as,

$$\tilde{OA}_j(Q_j, \tilde{P}_1, \tilde{P}_2, \cdots, \tilde{P}_{n_{arx}}) = \frac{\tilde{n}_{hd}(Q_j)}{n_{arx}} + \frac{\tilde{n}_{hd}(Q_j)}{\sum_{k=1}^{n_{arx}} n_k^{req}} - \frac{\sum_{i=1}^{n_{arx}} \tilde{P}_i}{Q_j},$$

where $\tilde{n}_{hd}(Q_j)$ is the number of requests that can be resolved by anchor node $j$, with the transmission power $Q_j = \frac{4\pi n\left(\tilde{g}^{-1}(Q_j)\right)^3}{3d^3}$. $\sum_{i=1}^{n_{arx}} \tilde{P}_i$ is the sum of the transmission power of the neighboring sensor nodes. $n_k^{req}$ is the demand from the $k$th neighbor sensor nodes of anchor node $j$ with the current transmission power $Q_j$. Similarly, the utility function of the $i$-th sensor node by ANFIS is computed according to Eq. (4), i.e., the weighted sum of the residual energy $\left(\tilde{E}_i^{tl} - E_i P_i\right)$ and the ability of sensor node $i$ to get their location $\tilde{OS}_i(P_i, \tilde{Q}_1, \tilde{Q}_2, \cdots, \tilde{Q}_{n_{srx}})$,

$$U_L(P_i, \tilde{Q}_1, \tilde{Q}_2, \cdots, \tilde{Q}_{n_{srx}}) = w_{1i}\left(\tilde{E}_i^{tl} - E_i P_i\right) + w_{2i}\tilde{OS}_i(P_i, \tilde{Q}_1, \tilde{Q}_2, \cdots, \tilde{Q}_{n_{srx}}), \tag{4}$$

where $\tilde{E}_i^{tl}$, $\tilde{n}_{neig}(P_i)$ and $\sum_{j=1}^{n_{srx}} \tilde{Q}_j$ are the fuzzy variables denoting the current total residual energy in the $i$-th sensor node, the number of neighbor anchor nodes including 'one-hop' and 'two-hop' anchor nodes with the transmission power $P_i$, and the sum of the transmission power of neighboring anchor nodes, respectively. $\tilde{OS}_i(P_i, \tilde{Q}_1, \tilde{Q}_2, \cdots, \tilde{Q}_{n_{srx}})$ is the sensor nodes' ability to get their location, calculated by,

$$\tilde{OS}_i(P_i, \tilde{Q}_1, \tilde{Q}_2, \cdots, \tilde{Q}_{n_{srx}}) = \frac{\tilde{n}_{neig}(P_i)}{n_{srx}} - \frac{\sum_{j=1}^{n_{srx}} \tilde{Q}_j}{P_i}.$$

The detailed explanations of Eqs. (3) and (4) can be found in paper [42].

Next, we analyze the existence of a Stackelberg Nash Equilibrium for the proposed Adaptive EELA method by following the methodology of [5]. Some concepts and properties of fuzzy variables of [5] are recalled first for sake of readability, as they are employed later to prove the Nash equilibrium achieved by Adaptive EELA.

Let $(\Theta, p(\Theta), Pos)$ be the possibility space for a nonempty set $\Theta$, where $p(\Theta)$ is the power of $\Theta$ and $Pos$ a possibility measure. We define $A$ as a fuzzy event if it is in $p(\Theta)$ and $Pos(A)$ gives the possibility that the event A will occur.

Definition 1. *Let $\xi$ be a fuzzy variable, which is defined as a function from the possibility space $(\Theta, p(\Theta), Pos)$ to the set of real numbers, whose membership function is designed as [26],*

$$\mu_\xi(x) = Pos\{\theta \in \Theta | \xi(\theta) = x\},\ x \in \mathbb{R}. \tag{5}$$

Definition 2. *A fuzzy variable $\xi$ is non-negative, if $Pos(\xi < 0) = 0$ [18].*

Remark. *$Pos(A) = 0$ means that the event A will not occur.*

Lemma 1. *If $\xi_i (i = 1, 2, \cdots, n)$ are a collection of independent fuzzy variables, and $f_i : \mathbb{R} \to \mathbb{R} (i = 1, 2, \cdots, n)$ are a set of functions, then, $f_i(\xi_i)(i = 1, 2, \cdots, n)$ are also independent fuzzy variables [18].*

Lemma 2. *Assuming $\xi$ and $\eta$ are two independent fuzzy variables whose values are expected to be finite. With any number of a and b, there is [19],*

$$E[a\xi + b\eta] = aE[\xi] + bE[\eta]. \tag{6}$$

According to its strategy, the problem of transmission power allocation of the $j$-th anchor node $Q_j$ is an optimization problem shown in Eq. (7). All of the anchor nodes are not cooperative. In Proposition 1, it is proved that for every anchor node, there is the best response strategy, and the unique equilibrium point is computed.

$$\begin{aligned}\max_{Q_j} E\left[U_F(Q_j, \tilde{P}_1, \tilde{P}_2, \cdots, \tilde{P}_{n_{arx}})\right] &= E\left[w_{1j}\left(\tilde{E}_j^{tl} - C_j Q_j\right)\right. \\ &\left. + w_{2j}\left(\frac{\tilde{n}_{hd}(Q_j)}{n_{arx}} + \frac{\tilde{n}_{hd}(Q_j)}{\sum_{k=1}^{n_{arx}} n_k^{req}} - \frac{\sum_{i=1}^{n_{arx}} \tilde{P}_i}{Q_j}\right)\right],\end{aligned} \tag{7}$$

s.t.

$$\begin{aligned}&\tilde{E}_j^{tl}, \tilde{n}_{hd}(Q_j), \tilde{P}_i > 0, \\ &Q_j, n_{arx}, n_k^{req}, C_j > 0, \\ &w_{1j}, w_{2j} \in (0,1), \\ &w_{1j} + w_{2j} = 1.\end{aligned} \tag{8}$$

Remark. *The condition (8) is defined according to Definition 2.*

Proposition 1. *Let $Q_j$ be the j-th anchor node's policy, then its optimal transmission strategy, $Q_j^*$, is calculated as,*

$$Q_j^*(\tilde{P}_1, \tilde{P}_2, \cdots, \tilde{P}_{n_{arx}}) = \left(\frac{w_{2j}\sum_{i=1}^{n_{arx}} E[\tilde{P}_i]}{w_{1j}C_j - w_{2j}Z_j}\right)^{\frac{1}{2}}, \tag{9}$$

with $w_{1j},\ w_{2j} \in (0,1)$, $w_{1j} + w_{2j} = 1$ and

$$Pos\left(\left\{w_1 j \le \frac{Z_j}{C_j + Z_j}\right\}\right) = 0, \tag{10}$$

where

$$Z_j = \left(\frac{1}{n_{arx}} + \frac{1}{\sum_{k=1}^{n_{arx}} n_k^{req}}\right)\frac{\partial E\left[\tilde{n}_{hd}(Q_j)\right]}{\partial Q_j}.$$

Proof. The fuzzy variables $\tilde{E_j^{tl}}$, $\tilde{n}_{hd}(Q_j)$ and $\sum_{i=1}^{n_{arx}} \tilde{P}_i$ in the optimization problem are assumed all independent. Since Adaptive EELA is proposed to improve the energy efficiency for the localization in UWSNs, all variables are non-negative.

From Eq. (7), we get,

$$E[U_F(Q_j, \tilde{P}_1, \tilde{P}_2, \cdots, \tilde{P}_{n_{arx}})] = E\left[w_{1j}\left(\tilde{E}_j^{tl} - C_j Q_j\right) + w_{2j}\left(\frac{\tilde{n}_{hd}(Q_j)}{n_{arx}} + \frac{\tilde{n}_{hd}(Q_j)}{\sum_{k=1}^{n_{arx}} n_k^{req}} - \frac{\sum_{i=1}^{n_{arx}} \tilde{P}_i}{Q_j}\right)\right]. \tag{11}$$

By Lemmas 1 and 2, we obtain,

$$E[U_F(Q_j, \tilde{P}_1, \tilde{P}_2, \cdots, \tilde{P}_{n_{arx}})] = w_{2j}\left(\frac{1}{n_{arx}} + \frac{1}{\sum_{k=1}^{n_{arx}} n_k^{req}}\right)E[\tilde{n}_{hd}(Q_j)] + w_{1j}E[\tilde{E}_j^{tl}] - w_{1j}C_j Q_j - w_{2j}\frac{\sum_{k=1}^{n_{arx}} E[\tilde{P}_i]}{Q_j}. \tag{12}$$

Then, in order to find the optimal solution, we apply the first order partial derivative of $E[U_F(Q_j, \tilde{P}_1, \tilde{P}_2, \cdots, \tilde{P}_{n_{arx}})]$ regarding to the $j$-th ($j \in [1, N]$) anchor node, is

$$\frac{\partial E\left[U_F(Q_j, \tilde{P}_1, \tilde{P}_2, \cdots, \tilde{P}_{n_{arx}})\right]}{\partial Q_j} = -w_{1j}C_j + w_{2j}\frac{\sum_{i=1}^{n_{arx}} E[\tilde{P}_i]}{(Q_j)^2} + w_{2j}\left(\frac{1}{n_{arx}} + \frac{1}{\sum_{k=1}^{n_{arx}} n_k^{req}}\right)\frac{\partial E[\tilde{n}_{hd}(Q_j)]}{\partial Q_j}. \tag{13}$$

Let $\frac{\partial E\left[U_F(Q_j, \tilde{P}_1, \tilde{P}_2, \cdots, \tilde{P}_{n_{arx}})\right]}{\partial Q_j} = 0$, and denote the solution $Q_j^{'}(\tilde{P}_1, \tilde{P}_2, \cdots, \tilde{P}_{n_{arx}})$, then we obtain from (13),

$$Q_j^{'2}(\tilde{P}_1, \tilde{P}_2, \cdots, \tilde{P}_{n_{arx}}) = \frac{w_{2j}\sum_{i=1}^{n_{arx}} E[\tilde{P}_i]}{w_{1j}C_j - w_{2j}Z_j}, \tag{14}$$

where

$$Z_j = \left(\frac{1}{n_{arx}} + \frac{1}{\sum_{k=1}^{n_{arx}} n_k^{req}}\right)\frac{\partial E\left[\tilde{n}_{hd}(Q_j)\right]}{\partial Q_j}.$$

In order to guarantee the existence of $Q_j^{'}$, the condition $w_{1j}C_j - w_{2j}Z_j > 0$ should be satisfied. Since $w_{1j},\ w_{2j} \in (0, 1)$ and $w_{1j} + w_{2j} = 1$, according to Definition 1 and 2, we get the condition as,

$$Pos\left(\left\{w_1 j \leq \frac{Z_j}{C_j + Z_j}\right\}\right) = 0.$$

Since $E[\tilde{P}_i] > 0$ according to Definitions 1, 2 and $\frac{\partial E[\tilde{n}_{hd}(Q_j)]}{\partial Q_j} > 0$ [42], we get $Q_j^{'}(\tilde{P}_1, \tilde{P}_2, \cdots, \tilde{P}_{n_{arx}})$ as,

$$Q_j^{'}(\tilde{P}_1, \tilde{P}_2, \cdots, \tilde{P}_{n_{arx}}) = \left(\frac{w_{2j}\sum_{i=1}^{n_{arx}} E[\tilde{P}_i]}{w_{1j}C_j - w_{2j}Z_j}\right)^{\frac{1}{2}}. \tag{15}$$

Then, we apply the second order partial derivative of $E[U_F(Q_j, \tilde{P}_1, \tilde{P}_2, \cdots, \tilde{P}_{n_{arx}})]$, which is computed as,

$$\frac{\partial^2 E[U_F(Q_j, \tilde{P}_1, \tilde{P}_2, \cdots, \tilde{P}_{n_{arx}})]}{\partial Q_j^2} = \frac{-2w_{2j}\sum_{i=1}^{n_{arx}} E[\tilde{P}_i]}{Q_j^3} + w_{2j}\left(\frac{1}{n_{arx}} + \frac{1}{\sum_{k=1}^{n_{arx}} n_k^{req}}\right)\frac{\partial^2 E[\tilde{n}_{hd}(Q_j)]}{\partial Q_j^2}. \tag{16}$$

Since $\frac{\partial^2 E(\tilde{n}_{hd}(Q_j))}{\partial Q_j^2} < 0$ [42], the value of the second order partial derivative of $E[U_F(Q_j, \tilde{P}_1, \tilde{P}_2, \cdots, \tilde{P}_{n_{arx}})]$ is negative. Finally, the optimal value $Q_j^*(\tilde{P}_1, \tilde{P}_2, \cdots, \tilde{P}_{n_{arx}}) = Q_j^{'}(\tilde{P}_1, \tilde{P}_2, \cdots, \tilde{P}_{n_{arx}})$, can be computed by $\frac{\partial E\left[U_F(Q_j, \tilde{P}_1, \tilde{P}_2, \cdots, \tilde{P}_{n_{arx}})\right]}{\partial Q_j} = 0$. □

To achieve the strategy definition of the of $P_i$ (the $i$-th sensor node), the problem of transmission power allocation could be equal to the following optimization problem,

$$\max_{P_j} E\left[U_L(P_i, \tilde{Q}_1, \tilde{Q}_2, \cdots, \tilde{Q}_{n_{srx}})\right] = E\left[w_{1i}\left(\tilde{E}_i^{tl} - E_i P_i\right) + w_{2i}\left(\frac{\tilde{n}_{neig}(P_i)}{n_{srx}} - \frac{\sum_{j=1}^{n_{srx}} \tilde{Q}_j}{P_i}\right)\right], \tag{17}$$

s.t.

$$\begin{aligned} &\tilde{E}_i^{tl}, \tilde{n}_{neig}(P_i), \tilde{Q}_j > 0, \\ &E_i, P_i, n_{srx} > 0, \\ &w_{1i}, w_{2i} \in (0, 1), \\ &w_{1i} + w_{2i} = 1. \end{aligned} \tag{18}$$

Remark. *The condition* (18) *is obtained according to Definition 2.*

The existence and uniqueness of is defined in Proposition 2, in which the existence and uniqueness of the Nash equilibrium is implied.

Proposition 2. *Assuming $P_i$ is the strategy of the i-th sensor node. For each sensor node, the best response is,*

$$P_i^*(\tilde{Q}_1, \tilde{Q}_2, \cdots, \tilde{Q}_{srx}) = \left( \frac{w_{2i} \sum_{j=1}^{n_{srx}} E[\tilde{Q}_j]}{w_{1i} E_i - \frac{\partial E[\tilde{n}_{neig}(P_i)]}{\partial P_i} \frac{w_{2i}}{n_{srx}}} \right)^{\frac{1}{2}}, \tag{19}$$

*under the conditions that*

$$Pos\left( \left\{ w_{1i} \leq \frac{\frac{\partial E[\tilde{n}_{neig}(P_i)]}{\partial P_i} \frac{1}{n_{srx}}}{E_i + \frac{\partial E[\tilde{n}_{neig}(P_i)]}{\partial P_i} \frac{1}{n_{srx}}} \right\} \right) = 0. \tag{20}$$

Remark. *From [42], we know that $\frac{\partial E[\tilde{n}_{neig}(P_i)]}{\partial P_i} > 0$. The condition of Eq. (20) is obtained according to Definition 1 and 2, based on which the existence of $P_i^*(\tilde{Q}_1, \tilde{Q}_2, \cdots, \tilde{Q}_{srx})$ is guaranteed.*

Remark. *For the prove of Theorem 2, the steps are comparable to those in the proof of anchor nodes, hence omitted.*

### 3.4 Adaptive EELA

In this part, we describe the overall protocol for implementing the proposed Adaptive EELA method, which comprises offline and online phases, as follows.

- Offline Phase: We first introduce the process for collecting the training dataset. According to [24], the model trained by the generated synthetic data is able to generalize across new scenarios and can perform well in real deployed networks. Hence, in this paper, we collected the training data from different simulations by the NS-3 simulator which reflect the real underwater scenarios. The simulation settings can be found in Table 3. Specifically, we use the grid search strategy on utility function's weights, e.g., $w_1 \in \{0.05, 0.1, 0.15, \cdots, 0.95\}$ and $w_2 \in \{0.05, 0.1, 0.15, \cdots, 0.95\}$ for both anchor and sensor nodes. We record the weights which produce a good performance in simulations. The energy consumption is mainly considered metric for the selection of weights. Then, for each pair of good weights, we run 3000 simulation instances to collect the training data. For anchor nodes, the dataset includes the anchor node's total residual energy, the number of requests resolved by anchor nodes, the sum of neighboring sensor nodes' transmission power, the energy consumption, and so on. Similarly, the dataset of sensor nodes includes the sensor node's residual power, the neighboring anchor nodes number, the sum of the transmission power of the neighboring anchor nodes, the energy consumption, and so on. Finally, for anchor / sensor nodes, we select 78000 samples with good performance, i.e., low energy consumption, to construct the fuzzy rules as well as membership functions of the sensor and anchor nodes' ANFIS. The trained ANFIS models are further employed as the utility functions of Stackelberg game. The training process is only needed once, which is described in detail in Fig. 3.
- Online Phase: In this stage, firstly, each node collects the environmental information, such as the residual energy and number of neighboring nodes, from its own and its neighboring nodes. The value of its optimal transmission power can be calculated by the trained Adaptive EELA model. Then, using the optimal transmission power, the sensor node sends the 'Request' message and when an anchor node receives 'Request' messages, it calculates the optimal transmission power by its trained Adaptive EELA model as well. The sensor node and anchor node use different trained Adaptive EELA models, respectively. When the sensor nodes achieve enough information from

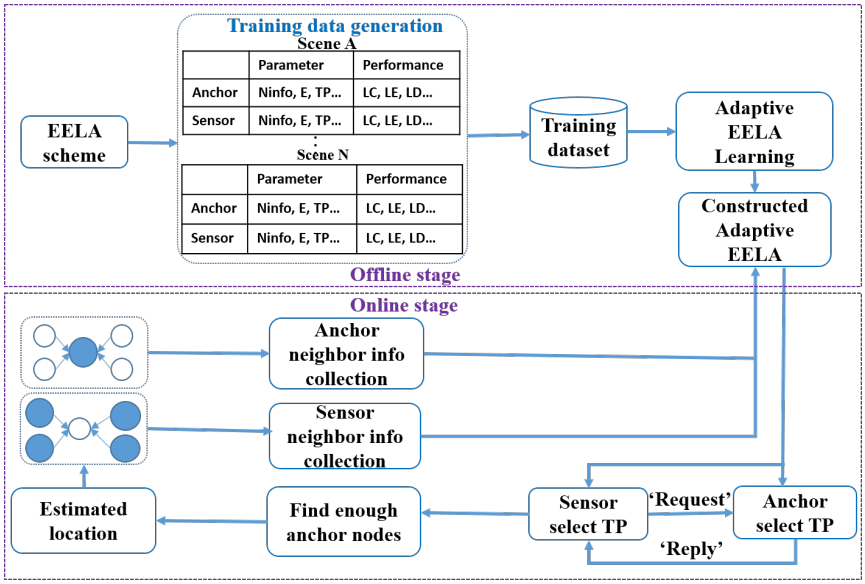


Fig. 3. Architecture of the proposed Adaptive EELA scheme.

anchor nodes, the localization process is carried out by trilateration or other localization algorithms. Details are illustrated in Fig. 3.

As for the algorithm design of Adaptive EELA, the general steps are similar to those of EELA [42]. It includes four steps, i.e., (1) anchor nodes broadcasting 'Wakeup' message, (2) anchor nodes broadcasting neighbor anchor list, (3) sensor nodes selecting optimal strategies, (4) anchor nodes selecting the optimal strategy based on the strategy of sensor nodes. After receive enough 'Reply' messages, the sensor nodes obtaining their locations. However, the key differences between Adaptive EELA and EELA are that Adaptive EELA employs ANFIS at both sensor and anchor nodes to determine their utility function instead of mathematically defined static functions. This avoids weights selected manually and enables all nodes to adapt to dynamic environmental changes and to learn the varying the relationship among the different factors, such as remaining energy, transmission power or neighboring nodes.

## 4 NUMERICAL EVALUATIONS

### 4.1 Simulation Settings

NS-3 [28] simulation platform is used to evaluate the proposed model. To inspect the online adaptation capability of Adaptive EELA, three simulation scenes are set considering different network topologies, A, B(a) and B(b), where B(a) and B(b) only differ in the number of sensor / anchor nodes. They are given in Table 2. Randomly, all of the sensor / anchor nodes are deployed beneath / on the surface. The transmission range takes continuous values in the scope of $(min\_range, max\_range]$ We have three inputs, five layers and eight rules for ANFIS method. The training epochs are 45. The other parameters including error tolerance and squash factor list in Table 2.

NS-3 UAN schemes are used as they provide various underwater network scenarios including three main parts: propagation, PHY and MAC. In particular, UanPhyGen model can use the distance to alter the transmission power, which is employed as the physical layer while UanMacCw model [30] is used as the MAC layer. It is remarkable that

Table 2. Different network scenes for the performance evaluation of schemes.

| Scene | Sensor Type | Nodes number | Simulation Area | $max\_range$ | $min\_range$ | Ocean Speed |
|---|---|---|---|---|---|---|
| A | anchor node<br>sensor node | 4<br>{10, 20, 30, 40, 50} | $2500^3 m^3$ | $\sqrt{2500^2 \times 3}$ | $\frac{max\_range}{2}$ | $\{2, 3, 4\,\mathrm{m\,s^{-1}}\}$ |
| B(a) | anchor node<br>sensor node | 20<br>{10, 20, 30, 40, 50} | $10000^2 m^2 \times 2500m$ | 5000 m | 2500 m | $\{2, 3, 4\,\mathrm{m\,s^{-1}}\}$ |
| B(b) | anchor node<br>sensor node | {4, 8, 12, 16, 20}<br>50 | $10000^2 m^2 \times 2500m$ | 5000 m | 2500 m | $\{2, 3, 4\,\mathrm{m\,s^{-1}}\}$ |

| Parameter | Value |
|---|---|
| Node mobility ($v_m$) | $2 - 4\ m/s$ |
| Node mobility model | Meandering Current Mobility model [4] |
| Channel Frequency | $22\ KHz$ [25] |
| Modulation technique | $FSK$ [25] |
| Data rate | $500\ bps$ [25] |
| Sound speed | $1500\ m/s$ [25] |
| Wave transmisson model | Thorp's propagation model [2] |
| Receive and Idle power | $0.1\ watts$ |
| Sleep power | $1 \times 10^{-4}\ watts$ |
| Range of influence | 0.5 |
| Squash factor | 1.25 |
| Accept ratio | 0.5 |
| Reject ratio | 0.15 |
| Error Tolerance | $1\times 10^{-6}$ |

Table 3. Simulation parameters.

although a collision avoidance mechanism is provided by UanMacCw model, collisions are still inevitable due to the problem of hidden / exposed nodes. In this study, UanPropModelThorp [3] is chosen as the propagation model while AcousticModemEnergyModel [8] is selected as the energy model. Table 3 illustrates the main simulation parameters.

In the simulation procedure, one node is localized after the reception of $n_{min}^{req}$ replies from anchor nodes. As the main goal is to improve the energy efficiency during the localization process rather than the design of a new localization algorithm, we use the well-known trilateration technique for localization, as an example to illustrate the performance of the proposed Adaptive EELA. In the trilateration technique, three anchor nodes are needed for a sensor node to locate itself, i.e., $n_{min}^{req} = 3$. All simulation results are averaged over 1000 runs. The movement of all nodes depends on the ocean current speed, according to the Meandering Current Mobility (MCM) model [4]. In such a model, the influence of the vortices as well as meandering sub-surface currents to the mobility of the nodes is considered.

### 4.2 Baseline Schemes

In the Adaptive EELA scheme, based on the fuzzy control algorithm, the transmission power of all nodes is able to be adjusted. Its performance is evaluated by comparison with seven baseline schemes listed below.

1) Ideal-EELA: The transmission power of all nodes is able to be adjusted according to utility functions defined in Eqs. (3) and (4). Weights are selected off-line by brute-force search.
2) EELA-Min: The fixed minimum transmission power, i.e., minimum transmission power, is used by all nodes.

3) EELA-Max: The fixed maximum transmission power, i.e., maximum transmission power is used by both sensor and anchor nodes.
4) Fixed-EELA [42]: The transmission power of all nodes is able to be adjusted according to utility functions calculated as Eq. (3) and (4). The weights in utility functions are fixed.
5) OLTC [25]: Only the transmission power of anchor nodes could be adjusted. The maximum transmission power is always utilized by sensor nodes.
6) 3DUL-Min [14]: The 3D localization scheme is first initiated by several surface anchor nodes. Sensor nodes that obtained their locations successfully can be switched to anchor nodes and these anchor nodes can further help more sensor nodes. The iteration continues until all sensor nodes obtaining their locations. All nodes broadcast messages by the fixed minimal transmission range.
7) 3DUL-Max [14]: The design steps are the same with those in 3DUL-Min but all nodes broadcast messages by the fixed maximal transmission range.

### 4.3 Performance Metrics

In order to verify all aforementioned methods' performance, the following metrics are used.

1) Localization coverage: the proportion of the number of localized sensor nodes to the entire number of sensor nodes.
2) Average energy cost of each node: the proportion of the entire energy cost to the number of all sensor and anchor nodes, given as,
$$\varepsilon_{total}^{avg} = \frac{\sum_{i=1}^{|\{N_s\}|}\varepsilon_i + \sum_{j=1}^{|\{N_a\}|}\varepsilon_j}{|\{N_s\}| + |\{N_a\}|}.$$
3) Average localization error: average distance between true location and predicted location computed as,
$$\frac{\sum_{i=1}^{|N_{sn\_l}|}\sqrt{(x_i - x_i^{'})^2 + (y_i - y_i^{'})^2 + (z_i - z_i^{'})^2}}{|N_{sn\_l}|}, \tag{21}$$
for an localized sensor node $i$, $(x_i,\ y_i,\ z_i)$ is the true location while $(x_i',\ y_i',\ z_i')$ is the predicted locations.
4) Average localization delay: the time duration since the broadcasting of a 'Request' message from a sensor node to the reception of its location.

### 4.4 Results and Analysis

The different network simulation scenes are given in Table 2 to prove the performance of Adaptive EELA. The current speed is set as $2\,\mathrm{m\,s^{-1}}$.

*4.4.1 Localization Coverage.* Firstly, the mean localization coverage over the number of sensor / anchor nodes in scenes A, B(a) and B(b) is evaluated (Table 2). Overall, from Fig. 4, it can be seen that the average localization coverage of EELA-Min is the lowest. The reason is that in this model, the minimum transmission range is used by both sensor and anchor nodes to send 'Request' and 'Reply' messages. There are no or only a few neighbors are discovered. Therefore, most sensor nodes can not obtain enough beacon information to calculate their locations in this design scheme. On the contrary, the average localization coverage in EELA-Max and 3DUL-Max achieve a good performance. 3DUL-Max even performs better than EELA-Max in some scenarios, e.g., scene B(b). This advantage is more obvious when there are only

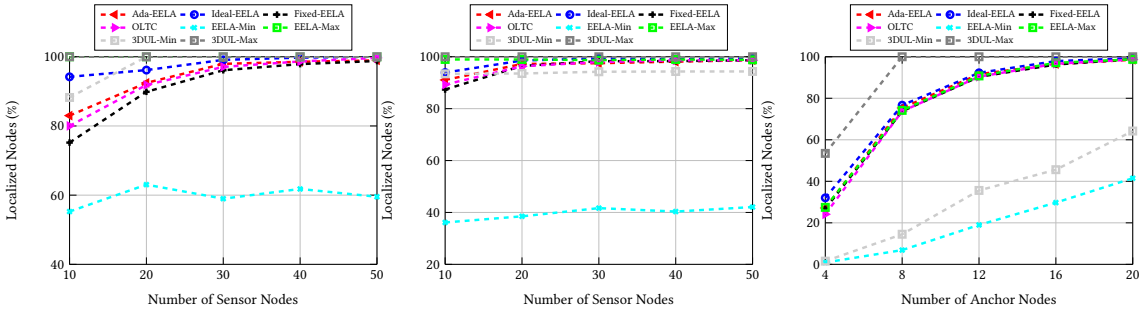


(a) Scene A. (b) Scene B(a). (c) Scene B(b).

Fig. 4. Localization coverage over various scenes.

a few sensor nodes. However, the energy cost of nodes by using a maximum transmission range is much higher, which is discussed in Section 4.4.2. It is also observed that, in terms of the average localization coverage, the performance of Ideal-EELA is better than Adaptive EELA, Fixed-EELA and OLTC while Adaptive EELA is better than Fixed-EELA and OLTC. The reason is that in Ideal-EELA, the best weights in utility functions are employed, which help both sensor and anchor nodes in selecting the optimal transmission ranges. In Adaptive EELA, each sensor node is adapted dynamically to different scenes and an optimal transmission range $R_i \leq R_{max}$ is select. Thereby we enable sensor nodes to reach the maximum number of anchor nodes while consuming minimum energy. Similarly, the optimal transmission ranges are also used by anchor nodes to send the 'reply' messages. For both sensor and anchor nodes, the optimal transmission ranges are selected based on the Stackelberg Nash Equilibrium as described in Section 3.3, i.e., all nodes are not able to improve the individual profit through altering the transmission range single-sidedly.

In Fig. 4(a) and 4(b), when we have a small set of sensor nodes, the localization coverage of Fixed-EELA and OLTC is slightly lower compared with Adaptive EELA. With more sensor nodes being deployed, the performance of them is close. In Fig. 4(c), the average localization coverage of Ada-EELA, Fixed-EELA, OLTC, and Ideal-EELA is close to that of EELA-Max and has the same trend due to the fixed number of sensor nodes. In addition, in Fig. 4(a) and 4(b), we observe that increase the number of sensor nodes improves the localization coverage of most schemes. Since the higher number of sensor nodes leads to the increase of the transmission range of anchor nodes, which further improves the localization coverage.

*4.4.2 Average Energy Cost.* The simulation results regarding the average energy cost for each node in different scenes are shown in Fig. 5.

As expected, EELA-Min and 3DUL-Min consume the lowest energy while EELA-Max and 3DUL-Max have higher energy consumption. The energy cost of 3DUL-Max is the highest due to its iterative localization strategy. We notice that the performance of Adaptive EELA and Ideal-EELA is closed while Fixed-EELA and OLTC have a higher energy cost. The reason is that Fixed-EELA cannot adapt to the environment because the fixed weights while OLTC always employs the maximum transmission range for sensor nodes, which consumes more energy.

The simulation scene A's results are illustrated in Fig. 5(a). The energy consumption in Adaptive EELA is about 35% and 66% reduced than Fixed-EELA and OLTC. In Fixed-EELA, anchor nodes are not able to achieve a good trade-off between the consumption of energy and the desired localization of sensor nodes. Similarly, sensor nodes cannot achieve a good balance, in which both energy cost and the capacity of finding anchor nodes are both needed to be satisfied.

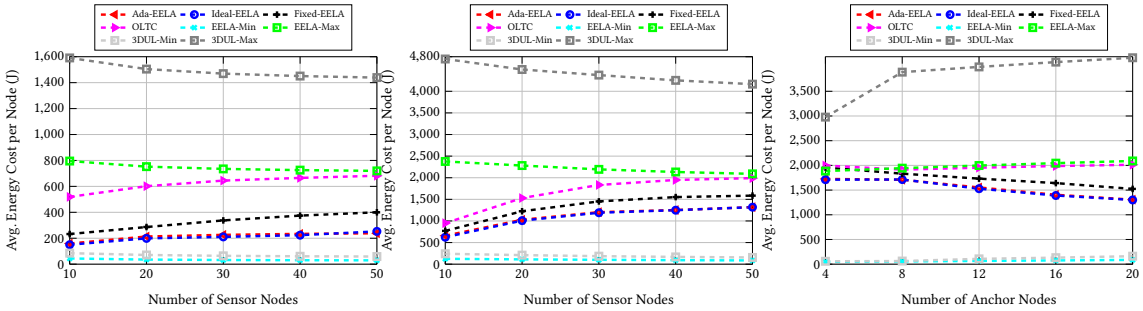


(a) Scene A. (a) Scene B(a). (c) Scene B(b).

Fig. 5. Average energy cost for each node over various scenes.

In OLTC, the maximum transmission range is used by sensor nodes to send 'Request' messages. This is the biggest portion of the energy consumed in the whole model. It is notable that in Adaptive EELA, to achieve the 'two-hop' anchor nearby nodes list, for anchor nodes, it is required to broadcast twice, which leads to about 30% higher average energy consumption for each anchor node in Adaptive EELA than OLTC. Nonetheless, in Adaptive EELA, the average energy cost for each sensor node is only about $\frac{1}{3}$ of OLTC. In localization systems, there are always many more sensor nodes than anchor nodes. This means that, despite the necessity of twice broadcast of anchor nodes, Adaptive EELA would save more energy than OLTC, on the whole. As for Ideal-EELA, since each scene is characterized by different density and topology of nodes, optimized weights according to scenes are employed. Therefore, its energy consumption for every node is the least, but a time-consuming offline weight optimization for each scene is inevitable.

The average energy cost over the number of sensor or anchor nodes is shown in Fig. 5(b). The major trends are similar to those observed in Fig. 5(a). Besides, we can see that for Ada-EELA, Fixed-EELA, Ideal-EELA, and OLTC, the consumed energy rises with the number of sensor nodes increasing, since both the average energy consumption per sensor node and anchor node increase. Meanwhile, the energy cost for each anchor node also increases as anchor nodes receive more 'Request' messages, making them select a larger transmission power for sending 'Reply' messages, as shown by the utility functions in Eq. (3).

Next, Fig. 5(c) depicts the average energy cost for each node over different sets of anchor nodes for scene B(b). Obviously, in Adaptive EELA, the energy cost of each node is about 13% and 23% less than Fixed-EELA and OLTC. In Eq. (4), we can see that the transmission range of sensor nodes is lowered when the density of anchor nodes is higher and eventually, the reduction of consumed average energy for each node. Moreover, more anchor nodes lead to higher average energy consumption for each node in EELA-Min, EELA-Max, and OLTC. The results can be explained as the fixed transmission range in these methods is used by sensor nodes. With more anchor nodes, due to higher consumption of energy by anchor nodes than sensor nodes, the average energy consumption for each node is higher. By contrast, the average energy cost for each node in Fixed-EELA, Ada-EELA, and Ideal-EELA decreases since sensor nodes use less transmission power if there are more anchor nodes around them, given the nature of utility functions of sensor node (see Eq. (4)). Furthermore, according to the utility functions of anchor nodes (see Eq. (3)), each anchor node receives less 'Request' messages and can hence consume less transmission power to send 'Reply' messages. Finally, it is worth noting that the energy consumption in Ada-EELA is significantly less than OLTC and Fixed-EELA.

*4.4.3 Average Localization Delay and Error.* Table 4 and 5 illustrates the average localization delay and error against the number of all nodes for each scene, respectively. In Table 4, we can see that the average localization delay of

| Scene | Adaptive EELA | Ideal-EELA | Fixed-EELA [42] | OLTC [25] | EELA-Min | EELA-Max | 3DUL-Min [14] | 3DUL-Max [14] |
|---|---|---|---|---|---|---|---|---|
| A | 6.11 | 5.86 | 6.88 | 6.80 | 5.41 | 6.95 | 8.41 | 9.27 |
| B(a) | 26.64 | 27.49 | 27.65 | 27.43 | 23.12 | 30.64 | 30.83 | 40.86 |
| B(b) | 7.89 | 7.86 | 7.87 | 7.67 | 5.77 | 7.77 | 7.39 | 10.36 |

Table 4. Average localization delay [s].

| Scene | Adaptive EELA | Ideal-EELA | Fixed-EELA [42] | OLTC [25] | EELA-Min | EELA-Max | 3DUL-Min [14] | 3DUL-Max [14] |
|---|---|---|---|---|---|---|---|---|
| A | 3.15 | 3.20 | 3.23 | 3.20 | 3.24 | 3.33 | 3.34 | 3.88 |
| B(a) | 3.75 | 3.99 | 4.18 | 3.71 | 3.84 | 3.62 | 5.12 | 6.83 |
| B(b) | 3.17 | 3.26 | 3.14 | 3.25 | 3.22 | 3.19 | 4.29 | 5.72 |

Table 5. Average localization error [m].

Adaptive EELA, Ideal-EELA, Fixed-EELA, and OLTC are close. EELA-Min has the lowest delay due to its minimum transmission range leading to fewer collisions in the channel while EELA-Max causes a longer delay. For 3DUL-Min and 3DUL-Max, the delays are accumulated over time because of their iterative localization strategy. In addition, the scene B(a) shows a high localization delay compared with other scenes, since the high number anchor nodes lead to high collision probability, which further results in the high delay.

In general, the performance of all algorithms except 3DUL in different scenes are close to each other in terms of localization error in Table 5. Since the trilateration technique is used for localization, three beacon locations, and accordingly, three values of a distance of anchor nodes are needed by each sensor node. With the broadcast of their precise coordinates from anchor nodes, the localization error caused by nodes' movement has a close relationship with the distance between sensor nodes and anchor nodes. 3DUL has a higher localization error because it has longer localization delay and the iterative strategy make the error increases accumulatively.

Overall, the proposed Adaptive EELA method enables the desirable trade-off levels among localization coverage, energy consumption, error, and delay, by successfully learning the dynamic environmental fluctuations thanks to the proposed Adaptive EELA scheme.

## 5 CONCLUSION

In this work, we present an adaptive fuzzy game-theoretic topology control method, Adaptive EELA, for achieving a high localization performance with low energy cost. The proposed Adaptive EELA method consists of two phases: the offline phase enables accurate training of the fuzzy neural network, while the online phase performs adaptive localization in the dynamic changing network environments. Based on the fuzzy optimization knowledge, the proposed fuzzy game is proven to reach Nash Equilibrium. Numerical results show that the proposed Adaptive EELA method enables remarkable trade-offs among localization coverage, amount of consumed energy, error and delay, compared to baseline methods, in various network environments. In different situations of UWSNs, the battery-limited sensor nodes are deeply deployed under the water, making them very difficult to replace or recharge. By contrast, anchor nodes are commonly set up on the water surface due to their convenience to be recharged or replaced. Hence, the proposed Adaptive EELA is well-suited for real-world implementation.

For the following research, the multi-path propagation issue by acoustic wave reflections, temperature or salinity of the water will be considered, based on which this Adaptive EELA method could be enhanced towards future applications.

## ACKNOWLEDGMENT

This project has received funding from the European Union's Horizon 2020 COSAFE project under grant agreement No 824019. We thank Megumi Kaneko for her helpful suggestions and feedbacks.

## REFERENCES

[1] Zaiwar Ali, Lei Jiao, Thar Baker, Ghulam Abbas, Ziaul Haq Abbas, and Sadia Khaf. 2019. A Deep Learning Approach for Energy Efficient Computational Offloading in Mobile Edge Computing. *IEEE Access* 7 (2019), 149623–149633.

[2] LM Brekhovskikh and Yu P Lysanov. [n. d.]. Theoretical Fundamentals of Ocean Acoustics [in Russian], Gidrometeoizdat, Leningrad (1982). *Google Scholar* ([n. d.]).

[3] Leonid Maksimovich Brekhovskikh, Yu P Lysanov, and Robert T Beyer. 1991. Fundamentals of ocean acoustics. *The Journal of the Acoustical Society of America* 90, 6 (1991), 3382–3383.

[4] Antonio Caruso, Francesco Paparella, Luiz Filipe M Vieira, Melike Erol, and Mario Gerla. 2008. The meandering current mobility model and its impact on underwater mobile sensor networks. In *INFOCOM 2008. The 27th Conference on Computer Communications. IEEE*. IEEE, 221–225.

[5] Fi-John Chang and Ya-Ting Chang. 2006. Adaptive neuro-fuzzy inference system for prediction of water level in reservoir. *Advances in water resources* 29, 1 (2006), 1–10.

[6] Valerio Di Valerio, Francesco Lo Presti, Chiara Petrioli, Luigi Picari, Daniele Spaccini, and Stefano Basagni. 2019. CARMA: Channel-aware reinforcement learning-based multi-path adaptive routing for underwater wireless sensor networks. *IEEE Journal on Selected Areas in Communications* 37, 11 (2019), 2634–2647.

[7] M Figueiredo and F Gomide. 1997. Adaptive neuro-fuzzy modeling. In *Fuzzy Systems, 1997., Proceedings of the Sixth IEEE International Conference on*, Vol. 3. IEEE, 1567–1572.

[8] Lee Freitag, Matthew Grund, Sandipa Singh, James Partan, Peter Koski, and Keenan Ball. 2005. The WHOI micro-modem: An acoustic communications and navigation system for multiple platforms. In *OCEANS, 2005. Proceedings of MTS/IEEE*. IEEE, 1086–1092.

[9] Zijun Gong, Cheng Li, and Fan Jiang. 2018. AUV-aided joint localization and time synchronization for underwater acoustic sensor networks. *IEEE Signal Processing Letters* 25, 4 (2018), 477–481.

[10] Zijun Gong, Cheng Li, Fan Jiang, and Jun Zheng. 2020. AUV-Aided Localization of Underwater Acoustic Devices Based on Doppler Shift Measurements. *IEEE Transactions on Wireless Communications* 19, 4 (2020), 2226–2239.

[11] Guangjie Han, Chenyu Zhang, Lei Shu, and Joel JPC Rodrigues. 2015. Impacts of deployment strategies on localization performance in underwater acoustic sensor networks. *IEEE Transactions on Industrial Electronics* 62, 3 (2015), 1725–1733.

[12] Albert F Harris III and Michele Zorzi. 2007. Modeling the underwater acoustic channel in ns2. In *Proceedings of the 2nd international conference on Performance evaluation methodologies and tools*. ICST (Institute for Computer Sciences, Social-Informatics and Telecommunications Engineering), 18.

[13] Gokhan Isbitiren and Ozgur B Akan. 2011. Three-dimensional underwater target tracking with acoustic sensor networks. *IEEE Transactions on Vehicular Technology* 60, 8 (2011), 3897–3906.

[14] M Talha Isik and Ozgur B Akan. 2009. A three dimensional localization algorithm for underwater acoustic sensor networks. *IEEE Transactions on Wireless Communications* 8, 9 (2009), 4457–4463.

[15] J-SR Jang. 1993. ANFIS: adaptive-network-based fuzzy inference system. *IEEE transactions on systems, man, and cybernetics* 23, 3 (1993), 665–685.

[16] Deying Li, Xiaohua Jia, and Hongwei Du. 2006. QoS topology control for nonhomogenous ad hoc wireless networks. *EURASIP Journal on Wireless Communications and Networking* 2006, 2 (2006), 43–43.

[17] Ning Li, Jennifer C Hou, and Lui Sha. 2005. Design and analysis of an MST-based topology control algorithm. *IEEE Transactions on Wireless Communications* 4, 3 (2005), 1195–1206.

[18] B Liu. [n. d.]. Theory and practice of uncertain programming, 2002. *Incorporated: Springer Publishing Company* 2 ([n. d.]).

[19] Baoding Liu and Yian-Kui Liu. 2002. Expected value of fuzzy variable and fuzzy expected value models. *IEEE transactions on Fuzzy Systems* 10, 4 (2002), 445–450.

[20] Linfeng Liu, Ye Liu, and Ningshen Zhang. 2014. A complex network approach to topology control problem in underwater acoustic sensor networks. *IEEE Transactions on Parallel and Distributed Systems* 25, 12 (2014), 3046–3055.

[21] Linfeng Liu, Ruchuan Wang, and Fu Xiao. 2012. Topology control algorithm for underwater wireless sensor networks using GPS-free mobile sensor nodes. *Journal of Network and Computer Applications* 35, 6 (2012), 1953–1963.

[22] Shukuan Liu and Zeshui Xu. 2014. Stackelberg game models between two competitive retailers in fuzzy decision environment. *Fuzzy Optimization and Decision Making* 13, 1 (2014), 33–48.

[23] Hanjiang Luo, Kaishun Wu, Yue-Jiao Gong, and Lionel M Ni. 2016. Localization for drifting restricted floating ocean sensor networks. *IEEE Transactions on Vehicular Technology* 65, 12 (2016), 9968–9981.

[24] Hongzi Mao, Ravi Netravali, and Mohammad Alizadeh. 2017. Neural adaptive video streaming with pensieve. In *Proceedings of the Conference of the ACM Special Interest Group on Data Communication (ACM SIGCOMM'17)*. 197–210.

[25] Sudip Misra, Tamoghna Ojha, and Ayan Mondal. 2015. Game-Theoretic Topology Controlfor Opportunistic Localization in Sparse Underwater Sensor Networks. *IEEE transactions on mobile computing* 14, 5 (2015), 990–1003.

[26] Steven Nahmias. 1978. Fuzzy variables. *Fuzzy sets and systems* 1, 2 (1978), 97–110.

[27] Zhaolong Ning, Jun Huang, Xiaojie Wang, Joel JPC Rodrigues, and Lei Guo. 2019. Mobile edge computing-enabled Internet of Vehicles: Toward energy-efficient scheduling. *IEEE Network* 33, 5 (2019), 198–205.

[28] nsnam.org. 2011. NS-3 Simulator. https://www.nsnam.org/. Online; accessed August 19, 2018.

[29] Erdal Panayirci, Mhd Tahssin Altabbaa, Murat Uysal, and H Vincent Poor. 2019. Sparse channel estimation for OFDM-based underwater acoustic systems in Rician fading with a new OMP-MAP algorithm. *IEEE Transactions on Signal Processing* 67, 6 (2019), 1550–1565.

[30] Nathan Parrish, Leonard Tracy, Sumit Roy, Payman Arabshahi, and Warren LJ Fox. 2008. System design considerations for undersea networks: Link and multiple access protocols. *IEEE Journal on Selected Areas in Communications* 26, 9 (2008).

[31] Hamid Ramezani, Fatemeh Fazel, Milica Stojanovic, and Geert Leus. 2015. Collision tolerant and collision free packet scheduling for underwater acoustic localization. *IEEE Transactions on wireless Communications* 14, 5 (2015), 2584–2595.

[32] Hongliang Ren and Max Q-H Meng. 2009. Game-theoretic modeling of joint topology control and power scheduling for wireless heterogeneous sensor networks. *IEEE Transactions on Automation Science and Engineering* 6, 4 (2009), 610–625.

[33] J Rezazadeh, M Moradi, K Sandrasegaran, and R Farahbakhsh. 2019. Transmission Power Adjustment Scheme for Mobile Beacon-Assisted Sensor Localization. *IEEE Transactions on Industrial Informatics* (2019).

[34] Nasir Saeed, Abdulkadir Celik, Tareq Y Al-Naffouri, and Mohamed-Slim Alouini. 2019. Localization of energy harvesting empowered underwater optical wireless sensor networks. *IEEE Transactions on Wireless Communications* 18, 5 (2019), 2652–2663.

[35] Nasir Saeed, Abdulkadir Celik, Tareq Y Al-Naffouri, and Mohamed-Slim Alouini. 2019. Underwater optical wireless communications, networking, and localization: A survey. *Ad Hoc Networks* 94 (2019), 101935.

[36] Hanif D Sherali, Allen L Soyster, and Frederic H Murphy. 1983. Stackelberg-Nash-Cournot equilibria: characterizations and computations. *Operations Research* 31, 2 (1983), 253–276.

[37] Robert Sutton and Paul J Craven. 1998. The ANFIS approach applied to AUV autopilot design. *Neural Computing & Applications* 7, 2 (1998), 131–140.

[38] Nazli Tekin and Vehbi Cagri Gungor. 2020. Analysis of compressive sensing and energy harvesting for wireless multimedia sensor networks. *Ad Hoc Networks* (2020), 102164.

[39] Jing Yan, Xiaoning Zhang, Xiaoyuan Luo, Yiyin Wang, Cailian Chen, and Xinping Guan. 2018. Asynchronous localization with mobility prediction for underwater acoustic sensor networks. *IEEE Transactions on Vehicular Technology* 67, 3 (2018), 2543–2556.

[40] Jing Yan, Haiyan Zhao, Xiaoyuan Luo, Yiyin Wang, Cailian Chen, and Xinping Guan. 2019. Asynchronous Localization of Underwater Target Using Consensus-Based Unscented Kalman Filtering. *IEEE Journal of Oceanic Engineering* (2019).

[41] Yali Yuan, Liuwei Huo, Zhixiao Wang, and Dieter Hogrefe. 2018. Secure APIT localization scheme against sybil attacks in distributed wireless sensor networks. *IEEE Access* 6 (2018), 27629–27636.

[42] Yali Yuan, Chencheng Liang, Megumi Kaneko, Xu Chen, and Dieter Hogrefe. 2019. Topology control for energy-efficient localization in mobile underwater sensor networks using Stackelberg game. *IEEE Transactions on Vehicular Technology* 68, 2 (2019), 1487–1500.

[43] Yali Yuan, Chencheng Liang, Megumi Kaneko, Lingjun Pu, and Xiaoming Fu. 2019. Adaptive Fuzzy Game-based Energy Efficient Localization in Underwater Sensor Networks. In *Proceedings of the ACM SIGCOMM 2019 Conference Posters and Demos*. 119–121.

[44] Yixin Zhang, Yuzhou Li, Yu Zhang, and Tao Jiang. 2018. Underwater Anchor-AUV Localization Geometries With an Isogradient Sound Speed Profile: A CRLB-Based Optimality Analysis. *IEEE Transactions on Wireless Communications* 17, 12 (2018), 8228–8238.

[45] Zhong Zhou, Jun-Hong Cui, and Shengli Zhou. 2010. Efficient localization for large-scale underwater sensor networks. *Ad Hoc Networks* 8, 3 (2010), 267–279.

[46] Jiang Zhu, Dingde Jiang, Shaowei Ba, and Yuping Zhang. 2017. A game-theoretic power control mechanism based on hidden Markov model in cognitive wireless sensor network with imperfect information. *Neurocomputing* 220 (2017), 76–83.